Cell. Mol. Life Sci. 65 (2008) 3918 – 3935
1420-682X/08/243918-18
DOI 10.1007/s00018-008-8590-4

Cellular and Molecular Life Sciences

Structure-function relationships in short-chain alcohol dehydrogenases

R. Ladenstein[a], J.-O. Winberg[b] and J. Benach[c,*]

[a] Karolinska Institutet NOVUM, Center for Structural Biochemistry, Hälsovägen 7 – 9, 14157 Huddinge (Sweden)
[b] Department of Medical Biochemistry, Institute of Medical Biology, Faculty of Medicine, University of Tromsø, 9037 Tromsø (Norway)
[c] ALBA Synchrotron Light Facility, Edifici de Ciències, Mòdul C-3 Central, Campus Universitat Autònoma de Barcelona, 08193 Bellaterra, Barcelona (Spain), Fax: +34-93-592-4302; e-mail: jbenach@cells.es

Online First 14 November 2008

Abstract. The structure-function relationships of alcohol dehydrogenases from the large family of short-chain dehydrogenase/reductase (SDR) enzymes are described. It seems that while mammals evolved with a medium-chain alcohol dehydrogenase family (MDR), fruit flies utilized an ancestral SDR enzyme. They have modified its function into an efficient alcohol dehydrogenase to aid them in colonizing the emerging ecological niches that appeared around 65 million years ago. To the scientific community, *Drosophila* has now served as a model organism for quite some time, and *Drosophila* alcohol dehydrogenase is one of the best-studied members of the SDR family. The availability of a number of high-resolution structures, accurate and thorough kinetic work, and careful theoretical calculations have enabled an understanding of the structure-function relationships of this metal-free alcohol dehydrogenase. In addition, these studies have given rise to various hypotheses about the mechanism of action of this enzyme and contribute to the detailed knowledge of the large superfamily of SDR enzymes.

Keywords. *Drosophila*, protein structure, x-ray crystallography, reaction mechanism, short-chain dehydrogenases/reductases, active site, alcohol dehydrogenase, kinetics.

Introduction

It is widely accepted that in early vertebrates, the medium-chain ethanol-oxidizing alcohol dehydrogenase ADH-I evolved from an ancestral ADH-III form, i.e. a glutathione-dependent formaldehyde dehydrogenase [1]. This enzyme is present in nearly all living organisms, and ADH 1 is a result of a duplication in osseous fish [2]. Perhaps this duplication was a requirement for the colonization of terrestrial habitats by vertebrates. However, much earlier, a similar ethanol-oxidizing system was produced within the order *Diptera* (from the Greek: *di* = two, and *pteron* = wing) or more commonly referred to as *flies*. This enzymatic system gave the flies and their larvae the opportunity to exploit sugar-rich but alas alcohol-sodden niches like rotting or fermenting fleshy fruits, which seem to have appeared at the same time [3] during evolution and probably favored fruit-fly speciation throughout the planet. In order to deal with the large amounts of alcohol, these flies came up with their own alcohol dehydrogenase version from an SDR (short-chain dehydrogenase/reductase) ancestor instead of an MDR (medium-chain dehydrogenase) ADH ancestor, even though an MDR-ADH-related enzyme was already present in the fruit flies, as an octanol dehydrogenase enzyme. The adaptability, simplicity, and relatively higher activity of the metal-free SDR proto-enzyme may have been evolutionarily favorable to the metabolism of the flies, which in turn had to endure and colonize highly diverse ecosystems

* Corresponding author.

Table 1. Sequence and kinetic data on several DADHs.

Enzyme[a]	Differences[b]	$k_{cat}(s^{-1})$[c]	References
D. simulans ADH	S1A, Q82K	1.9	[98]
Dm-ADH^{S}	–	3.4–4.0	[47, 99]
Dm-ADH$^{F'}$	A51D	4.0	[100]
Dm-ADH^{F}	K192T	10.4	[18, 40, 99–101]
Dm-ADH^{UF}	K192T, N8A, A45D	12–18	[18, 39, 101]
Dm-ADH^{FChD}	K192T, P214S	3.4[d]	[42]

[a]Labels represent Ds, *D. simulans*; Dm, *D. melanogaster*; S, slow; F, Fast; UF, ultrafast; FChD, fast (Château-Douglas).
[b]Primary sequence differences in relation to Dm-ADH^{S}. Numbering as in Dm-ADH.
[c]The catalytic center activities for 2-propanol, representing the dissociation rate of NADH from the enzyme-NADH complex, extracted from the references and from [102].
[d]From [103].

[4]. This evolutionary explosion resulted in more than 2000 fruit fly species (including the Drosophilidae and Tephritidae families) that during millions of years have spread throughout many habitats. These habitats can range from deserts to tropical rainforests and from cities to alpine zones, including many sorts of fruit and varying levels of alcohols of several types [5–8]. As far as we know, alcohol dehydrogenase of the fruit fly-type from both the Drosophilidae and Tephritidae families is the only member of the SDR family (ExPASy [9]) that is optimized to act exclusively on simple aliphatic alcohols (EC 1.1.1.1), like ethanol. Many members of the SDR family act on more bulky substrates, like steroids, prostaglandins, xenobiotics, and sugars.

Drosophila has been employed for quite some time as a laboratory model for genetics in general and also extending into human diseases. At least 75% of fruit-fly diseases, like substance addiction and Alzheimer's disease, have equivalents in humans [10, 11]. Furthermore, and practical these days, the small flies can be employed as a tool for monitoring global warming and climate change [12]. In this context, the alcohol dehydrogenase gene/enzyme system (*adh*-ADH) from *Drosophila* has been studied in great detail for the past several decades [11, 13–20]. *Drosophila* ADH (DADH) was found to be an NAD^+-dependent oxidoreductase (EC 1.1.1.1) and to belong to the SDR family [5, 15, 21–23]. DADH oxidizes small aliphatic alcohols to their respective aldehydes or ketones [24], and its function in energy metabolism and alcohol tolerance by the fruit flies, conferring fitness to them, has been documented [25]. This enzyme is also highly abundant in the flies, and it can be as much as 1–2% of the total soluble protein [15]. DADH is a clear example of how environmental factors may actually favor biochemical traits at the molecular level of key enzymatic proteins.

The thousands of species of fruit fly that populate the planet carry slightly different versions of the ADH enzyme. Some, like *Drosophila melanogaster* ADH, are present in nature in well-studied alleloforms, ADH-slow (Dm-ADH^{S}), ADH-fast (Dm-ADH^{F}), and ADH-ultrafast (Dm-ADH^{UF}), that display different kinetic properties and geographic distribution even though they vary only in a couple of amino acid residue differences far from the active or coenzyme binding sites. Other DADHs are thermostable, like ADH-Fast (Château-Douglas) (Dm-ADH^{FChD}) or Dm-ADH^{71k} (Table 1). The frequency of the *adh*-f allele increases at the expense of *adh*-s with increasing latitude in both hemispheres of the earth. Kinetic, genetic, structural, and biological information is limited among other SDR members, for which only a few representatives have been studied. DADH has also been found in different more or less inactive isoforms: DADH-3 and DADH-1. They are induced by addition of secondary alcohols/ketones to the food of the flies, or by incubation of crude enzyme extracts or purified enzymes with high amounts of NAD^+ and a ketone. Consequently, DADH-3 and DADH-1 isoforms are postulated to be reversible or irreversible forms of an enzyme ternary complex involving NAD^+ and a ketone [26]. Since the metabolism of *Drosophila* cannot further degrade ketones generated from secondary alcohols present in the food, accumulation of these ketones inhibits DADH activity. Thus, it would appear as if this enzyme has a path to auto-regulate its enzymatic function *in vivo*, by creation of abortive complexes with NAD^+ and ketones. Although the DADH-1 isoform is metabolically inert, it increases the *in vivo* half-life of the remaining DADH molecules by a factor of five [27].

Three-dimensional structure of fruit-fly ADH

Like MDR-ADH, DADH is active as a dimer and uses NAD^+ as co-enzyme to oxidize small aliphatic alco-

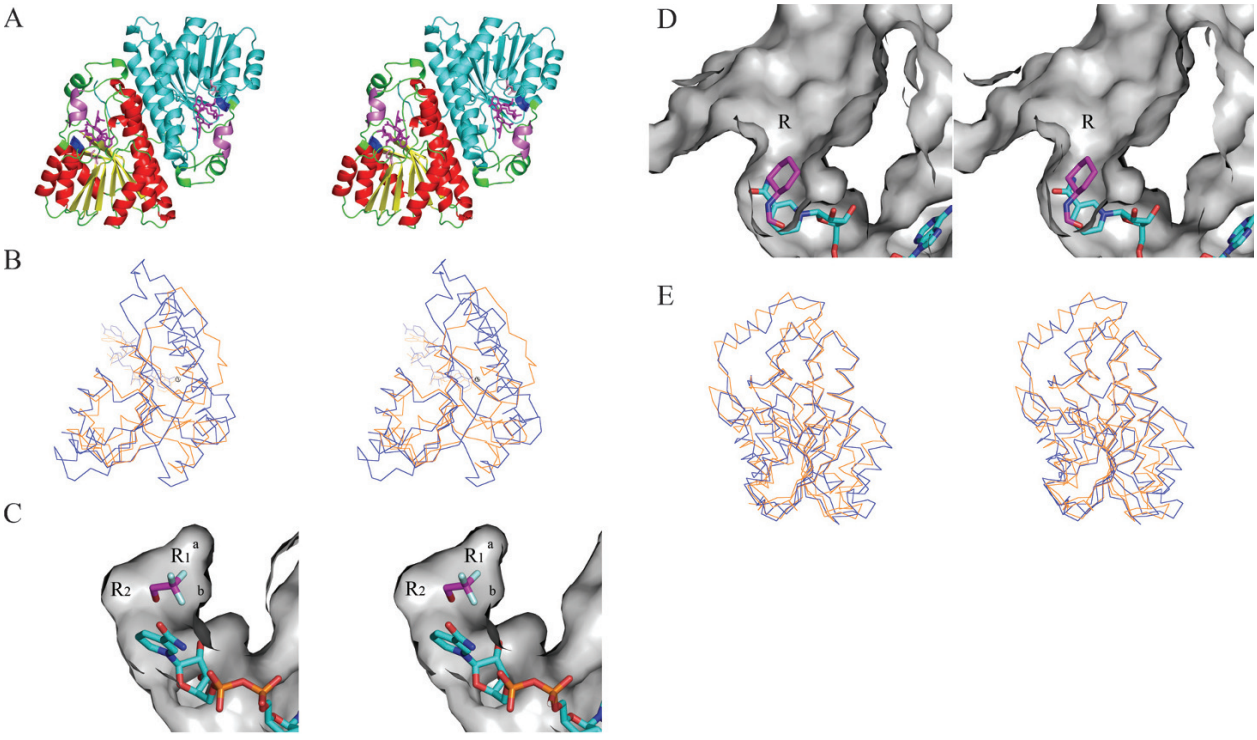

Figure 1. (*A*) A ribbon representation of a dimer of *D. lebanonensis* ADH complexed with NAD-3-pentanone [34] (PDB ID 1B16) is shown in stereo with one subunit colored by secondary structure elements (red: α-helices and yellow: β-strands) and the other subunit in cyan. Selected segments of the molecule are also colored to show their spatial relation with the ligand. The characteristic active site loop or *lid* is (one turn α-helix, turn, small α-helix) colored green, with the small stretch of residues (186–191) in violet, the glycine-rich loop (residues 15–17) is colored in blue, Asp37 in pink, and the ligand is shown in magenta. The two long α-helices correspond to αE and αF. (*B*) Stereo Cα superposition between the two overlapping domains (according to DALI [36]) that constitute the Rossmann fold. *D. lebanonensis* ADH complexed with NAD^+ (PDB ID 1B14) both in blue (residues 3–179), and horse liver ADH and NAD^+ in orange (PDB ID 1LDY) (residues 190–317). (*C*) Stereo-view of the solvent-accessible surface of the active site of *D. lebanonensis* ADH with 2,2,2-trifluoroethanol and NAD^+ (PDB ID 1SBY) with oxygen, nitrogen, and phosphorus atoms colored in red, blue, and orange, respectively, and the color of the carbon atoms depending on whether they belong to the inhibitor (magenta) or to NAD^+ (cyan). (*D*) Stereo view of the solvent-accessible surface of the active site of horse liver alcohol dehydrogenase complexed to NADH and cyclohexyl formamide [110] (PDB ID 1LDY), with oxygen, nitrogen, and phosphorus atoms in red, blue, and orange, respectively, and the color of the carbon atoms depending on whether they belong to the inhibitor (magenta) or to NADH (cyan). (*E*) Stereo Cα superposition between *D. lebanonensis* ADH complexed and NAD^+ (PDB ID 1B14) both in blue, and human 15-hydroxyprostaglandin dehydrogenase (PDB ID 2GDZ) in orange. This figure was created with PYMOL [111]. 3D superpositions were performed with SSM [112] in COOT [113].

hols, such as ethanol, into their corresponding aldehydes/ketones. Any mutation or modification that alters the quaternary structure of DADH abrogates enzymatic activity [28]. The similarities between MDR-ADH and SDR-ADH end here, since the two identical subunits in each case have different structures and family assignments [13, 29]. The most remarkable difference is the lack of metal in DADH. Once the three-dimensional structure of DADH was unveiled [30], it revealed an overall structure that was typical of SDRs: an α/β fold with a characteristic NAD(H)-binding motif or Rossmann domain [30–35] at the N terminus of the polypeptide chain (Fig. 1A). A monomer of DADH is folded into a central eight-stranded β-sheet and flanked on each side by three α-helices. The central β-sheet is created by seven parallel and one antiparallel β-strand. Because of the common Rossmann-fold derivation, the structures of DADH and horse liver ADH give a Z-score of 7.4 and an RMSD of 3.0 Å in DALI [36] for alignment of the 117 Cα atoms that form the residues sharing 15% sequence identity. The overlapping residues constitute mostly the coenzyme-binding domain or the N-terminal central β-sheet (Fig. 1B). Remarkably, the topology of this domain is largely conserved between these two enzyme families, despite their evolutionary differences. Since SDR-DADH shows a clearly different three-dimensional structure than that of MDR-ADH but the same enzymatic function, it is a clear example of convergent evolution in nature.

The crystal structure also showed that the two main components of the dimer interface are two elongated α-helices in each monomer, αE and αF. They wrap around the same helices from the other subunit (Fig. 1A). In a secondary role in this subunit interface, we find the active site loop and a rare motif in SDRs,

the last stretch of C-terminal residues in one subunit which help isolate the active site loop from the solvent in the other subunit and for which deletion results in the loss of enzymatic activity [37] (Fig. 1A). The interactions that form the quaternary structure are mostly hydrophobic, with no ion-pairs present and only a few hydrogen bond interactions. The large dimer interface and the nature of the interactions to create the dimer explain the dimeric nature of this enzyme for activity [28].

From the ternary and binary complexes, the conformation of the coenzyme bound to the enzyme can be determined. The oxidized or reduced coenzyme, NAD^+ [34] or NADH [32], binds to DADH in an extended conformation with the adenine ring in *anti* and the nicotinamide in *syn* conformation (Fig. 1B). The *syn* conformation of the nicotinamide ring suggests a B-face 4-pro-*S* hydride transfer reaction in contrast to the situation in MDR-ADH, where the hydride is transferred from the alcohol to the coenzyme via the A-face of the nicotinamide ring [34]. The phosphate moiety of the coenzyme interacts with the amide groups of the highly invariant glycine-rich loop (residues from Gly15 to Ile17, numbering as in *D. lebanonensis* ADH, unless noted otherwise) (Fig. 1A), a flexible region that is partly disordered in the *apo* form of the enzyme. An aspartic acid residue at position 37 (Fig. 1A) prevents DADH from using $NADP^+$ as coenzyme because of electrostatic repulsion between the side chain of the acidic residue and the extra phosphate group in the ribose near the adenine ring of $NADP^+$ [38].

The reaction mechanism of *Drosophila* ADH

DADHs reversibly convert short- and medium-chain primary and secondary alcohols to their corresponding aldehydes or ketones using NAD^+ as coenzyme [18, 39–42]. In addition, DADHs can also further oxidize aldehydes to carboxylic acids [43–45], which is, however, an essentially irreversible process.

Steady-state kinetic studies have shown that the *Drosophila* alcohol dehydrogenase reaction follows a Michaelis–Menten type of kinetics. Kinetic studies were consistent with an ordered reaction mechanism for the interconversion of primary/secondary alcohols and their corresponding aldehydes/ketones, as well as for the oxidation of aldehydes to their corresponding carboxylic acids [45–50]. In these reactions, the oxidized and reduced coenzymes, NAD^+ and NADH, respectively, bind to the free enzyme E, and the alcohol and aldehyde/ketone bind to the binary enzyme-NAD(H) complexes. This reaction mechanism is based on studies using alternative alcohols, aldehydes/ketones, and product and dead-end inhibitors.

The rate-limiting step of the reaction is determined by the type of substrate [18, 39–41, 47, 49]. With primary alcohols (like ethanol), the rate-limiting step is the hydride transfer in the ternary enzyme-NAD^+-alcohol complex. A primary isotope effect ($k_{cat}{}^{H}/k_{cat}{}^{D}$) of approximately 3 was obtained with ethanol, showing that the rate-limiting step is the hydride transfer. This rate-limiting step also explains the observed variation in the k_{cat} value for various primary alcohols.

In contrast, with most of the tested secondary alcohols, the breakdown of the ternary enzyme-NAD^+-alcohol complex is fast, and the rate-limiting step is then the release of NADH from the binary enzyme-NADH product complex. The k_{cat} value is approximately the same for most secondary alcohols, and this value is much higher than for primary alcohols. In addition, no primary isotope effect can be detected for the secondary alcohols propan-2-ol and cyclohexanol.

In the reverse reaction, the rate-limiting step for acetaldehyde reduction is mainly the dissociation of the binary enzyme-NAD^+ product complex [47, 49]. However, the reaction with acetone is much slower than that with acetaldehyde, and the rate-limiting step is either one or several of the preceding steps. Product inhibition studies also reveal that both acetaldehyde and acetone can form binary dead-end enzyme-aldehyde/ketone complexes [48].

In contrast to the situation with aldehydes, it is not possible to detect a ternary enzyme-NAD^+-acetone complex in product inhibitory studies [48]. However, several studies have shown that DADH forms a stable ternary enzyme-NAD^+-ketone complex [14, 34, 51, 52]. The electrophoretic mobility of this ternary complex is also largely changed towards the anode compared to the uncomplexed enzyme. This conversion of a DADH-5 electrophoretic variant (enzyme without bound NAD^+-ketone) to DADH-3 (an NAD^+-ketone bound to one subunit) and DADH-1 (an NAD^+-ketone bound to each subunit) variants may be an irreversibly or strongly reversibly bound complex between the enzyme and an NAD^+-ketone adduct, as it has not been possible to remove the coenzyme-ketone from the enzyme during extended dialysis. These results are supported by the crystal structures of DADH with several NAD-ketone adducts, obtained at different resolutions and crystallization conditions (Table 2) [34]. Inactivation kinetic studies show that a very weak reversible ternary enzyme-NAD^+-acetone complex ($K_{EO,A} = 1.7$ M) forms prior to the formation of a very strong reversible or irreversible ternary complex.

The substrate binding site of *Drosophila* ADH

The shape of the alcohol-binding site in the binary DADH-NAD^+ complex was suggested approximately

Table 2. Summary of all the DADHs available in the protein databank.

Organism	Ligand(s)	Resolution (Å)	PDB ID	References
D. lebanonensis	–	1.9	1A4U	[30]
D. lebanonensis	NAD^+	2.4	1B14	[34]
D. lebanonensis	NAD-acetone	2.2	1B15	[34]
D. lebanonensis	NAD-pentan-3-one	1.4	1B16	[34]
D. lebanonensis	NAD-cyclohexanone	1.6	1B2L	[34]
D. lebanonensis	NAD^+ and 2,2,2-trifluoroethanol	1.1	1SBY	
D. melanogaster	NADH and acetate	1.6	1MG5	[32]

Table 3. Structural homologs of DADH.[a]

Name	Organism	PDB ID:chain	RMSD (Å)	Sequence identity (%)	Equivalent positions	P-value	References
15-Hydroxyprostaglandin dehydrogenase type1	*Homo sapiens*	2GDZ:A	3.2	25.2	243	29.2	[55]
Clavulanic acid dehydrogenase	*Streptomyces clavuligerus*	2JAP:A	3.1	20.4	222	25.8	[56]
17β-hydroxysteroid dehydrogenase	*Homo sapiens*	1BHS:A	3.1	19.7	210	25.4	[105]
Mannitol 2-dehydrogenase	*Agaricus bisporus*	1H5Q:B	3.1	18.2	221	25.0	[104]
Trihydroxynaphthalene reductase	*Magnaporthe grisea*	1DOH:B	3.4	17.1	218	24.8	[106]
11β-hydroxysteroid dehydrogenase isozyme 1	*Homo sapiens*	1XU9:B	3.1	20.3	218	24.7	[107]
Glucose dehydrogenase	*Bacillus megaterium*	1GCO:B	3.2	19.3	213	24.7	[108]

[a]Data obtained using DBali [109] and the crystal structure of *D. lebanonensis* ADH complexed with NAD-3-pentanone (PDB ID 1B16) as search target.

20 years before the actual determination of its three-dimensional structure by x-ray crystallography. The reason for this is that the topology of the active site determines the substrate specificity of the enzyme. In substrate specificity studies of the three *D. melanogaster* alleloenzymes Dm-ADH^S, Dm-ADH^F, and Dm-ADH^{UF}, and *D. lebanonensis* ADH (Dl-ADH), approximately 100 structurally well-defined alcohols were employed [18, 39–41]. The kinetic coefficient that best describes the substrate specificity and the variation for ethanol and propan-2-ol shows the same variation with pH [47], and hence it was possible to compare substrate specificities from studies done at different pH values as shown in a previous review of DADHs [18].

Indeed, the active site/substrate binding cavity becomes much more well-ordered in the ternary complexes of DADH with coenzyme and inhibitors when compared to the *apo* or *holo* forms [30, 34]. This cavity is excluded from the solvent by the spatial ordering of a stretch of only six residues (186–191) and contains at its base the three active site residues that are postulated to be responsible for the reaction mechanism: Tyr151, Lys155, and Ser138 (Fig. 1A, C). This cavity is lined with the side chains of hydrophobic residues and retains its shape in all the available crystal structures of ternary complexes of DADH obtained so far (Table 2) [18, 39, 40] and, as hinted by kinetic studies [18, 39–41], can be divided into two asymmetrical sub-cavities (R_1, R_2) (Fig. 1C). This architecture of the active site explains why *R*-secondary alcohols are better substrates than *S*-secondary alcohols (Fig. 2A), and why most secondary alcohols are much better substrates than primary alcohols. The cavity seems to be too large for methanol to bind, and thus explains why DADH is not active with this alcohol. The crystal structure also shows that the shape and size of the R_1 sub-cavity, which can be further divided into R_1a and R_1b (Fig. 1C), when compared to R_2 also explains why bi-cyclic secondary alcohols R-(+)-cis-verbenol, R-(+)-trans-bicyclo(2.2.1)-heptanol, S-(−)-trans-bicyclo(2.2.1)-heptanol, and S-(−)-cis-bicyclo(2.2.1)-heptanol are much better substrates than the other three isomeric forms of verbenol or borneol (see Fig. 3). Supporting the hypothesis that the active site of DADH remains

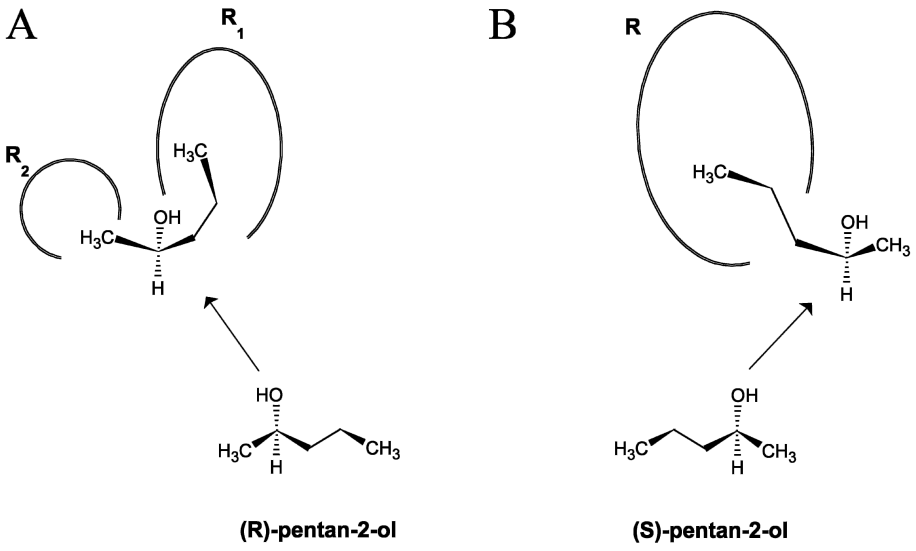

Figure 2. Schematic representation of the active-site cavities of DADH (*A*) and HLADH (*B*). As an example the two enantiomers of pentan-2-ol are shown in relation to the active site cavities. This figure was created with the free version of ACD/3D (Advanced Chemistry Development, Inc., Toronto, Ontario, Canada).

relatively rigid when binding to the substrates (except for the small stretch from residues 186–191 that seems to act as a gate for the substrate and is disordered in the *apo* form and partly ordered in the *holo* form of the enzyme), adjusted fits do not occur or are minimal during substrate binding.

Both kinetic and crystallographic data for Dl-ADH complexed with NAD-ketone adducts show that the alkyl chain of ethanol (in the oxidative reaction) and aldehydes (in the reductive reaction) bind to the R_1 part of the bifurcated alcohol binding site [34, 53, 54]. This results in transfer of the *pro-S* hydrogen in ethanol to the coenzyme. However, in the further oxidation of aldehydes to acids, the alkyl chain of the aldehyde binds to the R_2 part of the active site [32], a finding that supported the suggestion [43] that the *gem*-diol form of aldehydes binds to the binary enzyme-NAD^+ complex in the oxidation of an aldehyde to the corresponding carboxylic acid. The crystal structure data also indicate that one of the hydroxyl groups in the *gem*-diol are at hydrogen bonding distance to the hydroxyl group in the side chain of the active site Ser138 and Tyr51, while the other hydroxyl group points into the R_1b cavity close to the C7-amide group of the nicotinamide moiety of the coenzyme.

Comparison with other members of the SDR family

Comparison of the crystal structure of DADH with all the crystal structures currently available in the protein databank (PDB) (http://www.rcsb.org/pdb/) (Table 3) shows that the nearest structural homolog is human 15-hydroxyprostaglandin dehydrogenase type 1 (PDB ID 2GDZ) [55], an SDR enzyme involved in inflammation. In this protein, the active site loop (residues 185–220) contains a cavity that is structurally the closest to that of DADH (Fig. 1E). It is lined with hydrophobic residues as in DADH, but there are two significant differences. Thus, Val14 and Leu95 in DADH are substituted by Gln148 and Asn95 in 15-hydroxyprostaglandin dehydrogenase, respectively. These two changes and the fact that the cavity is filled with many well-ordered water molecules (in contrast to DADH which shows only one water molecule in the NAD^+-enzyme binary complex), show that specific changes preserving the overall topology of the active site loop are enough to change the affinity/activity from small/medium-sized secondary alcohols in DADH to much larger prostaglandins in 15-hydroxyprostaglandin dehydrogenase. The next closest structural homolog is clavulanic acid dehydrogenase (PDB ID 2JAP) from *Streptomyces clavuligerus*, which is responsible for the NAPDH-dependent reduction of the unstable intermediate clavulanate-9-aldehyde, which yields clavulanic acid [56], a β-lactamase inhibitor of importance in treatments of penicillin-resistant infections. This enzyme has an arginine (Arg208) pointing toward the middle of the active site cavity, a space that is also filled with many ordered water molecules. As expected, the introduction of a positively charged residue in the active site cavity accounts for the change in specificity of this enzyme towards the clavulanic acid molecule, which contains a negatively charged carboxylic group. The remaining structural homologs found in the PDB show an active site lid that departs considerably from that of DADH, thus explaining the difference in substrate specificity. A secondary element that seems to be largely conserved, by acting as a gate to the active site, is the small one-turn α-helix at the beginning of the loop

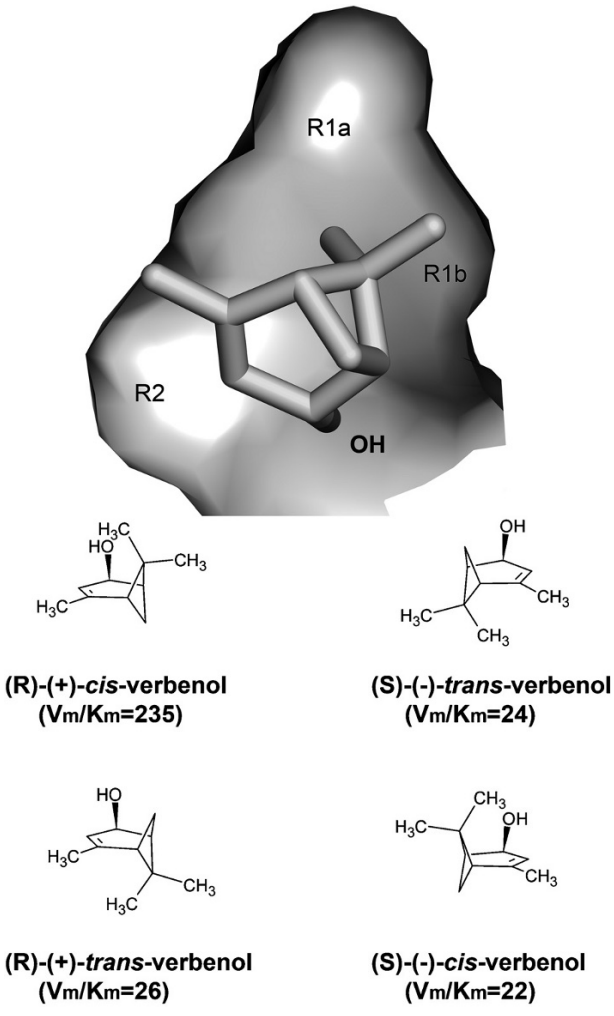

Figure 3. Active site cavity of DADH with a molecule of (*R*)-(+)-*cis*-verbenol modeled in it according to general chemical considerations to favor proton and hydride transfer (top) in gray and with the hydroxyl group of the molecule marked with an OH label. The chemical structures (below) show the four enantiomers of verbenol and under each name the value of V_m/K_m (a.u. x mM^{-1}) relative to ethanol (which corresponds to a V_m of 100 a.u.). From the three-dimensional structure, we can see that (*R*)-(+)-*cis*-verbenol is the only one to efficiently fit the active site cavity of DADH. Kinetic values taken from [39]. The structure of Dl-ADH complexed with 2,2,2-trifluoroethanol (PDB ID 1SBY) (Table 2) was used to generate the active site cavity. This figure was made with PYMOL [111] and ACD/3D (Advanced Chemistry Development, Inc., Toronto, Ontario, Canada).

(residues 186–191, Fig. 1A), which seems to be a feature necessary for the correct fold of the active site *lid* (Table 3). Similar active site *lids* in SDR enzymes (Fig. 1A, E, and the top two entries in Table 3) with unrelated catalytic activity reinforce the hypothesis that SDR-type alcohol dehydrogenase activity in *Drosophila* arises from an enzymatically unrelated SDR ancestor [57].

Comparison with medium-chain ADH

In contrast to the DADH specificity, primary alcohols are better substrates than secondary alcohols for liver MDR-ADH [58, 59], and the catalytic activity then increases with the alcohol chain length. One exception is cyclohexanol, which is oxidized with a rate that is comparable to that of ethanol [58, 60]. Stereospecificity is also different between horse liver ADH (HLADH) and DADH, as it is the *pro*-R hydrogen in ethanol that is transferred to NAD^+ [61–63]. These differences between DADH and liver ADH are clearly understood when examining the topology of the corresponding alcohol binding sites (Fig. 1C, D). As noted above, the active site cavity of DADH is asymmetrically bifurcated, explaining why this enzyme prefers secondary instead of primary alcohols. In the case of MDR-ADH, the active site cavity is more like an elongated funnel, and fully exposed to the solvent (Fig. 1D). Again, the latter shape explains why the medium-chain ADH prefers primary instead of secondary alcohols (Fig. 2B) and is also able to accommodate large and elongated substrates like steroids or even bile acids (Figs. 1D, 2).

pH dependence of the *Drosophila* ADH reaction

It was shown for the *D. melanogaster* ADH^S alleloenzyme and *D. lebanonensis* ADH that some of the kinetic coefficients for the oxidation of alcohols and for the reduction of acetaldehyde vary with pH [47, 49, 50, 64]. In addition, the pH dependence for the binding of pyrazole and 2,2,2-trifluoroethanol to the binary enzyme-NAD^+ complex has been studied in detail [47, 49, 50, 64]. In the compulsory ordered mechanism for both enzymes, k_{on} for NAD^+ increases and k_{on} for NADH decreases with increasing pH. It appears to be more than one amino acid residue that regulates the k_{on} velocity for the two coenzymes. The k_{cat} value for propan-2-ol does not vary with pH, which shows that k_{off} for NADH does not vary with pH. In contrast, k_{off} for NAD^+ increases with decreasing pH.

As for propan-2-ol, the k_{cat} value for ethanol does not vary with pH, and hence, this is also the case for the k (the hydride transfer step) constant. Neither does the kinetic coefficient ϕ_2' for the reduction of acetaldehyde vary within the pH region studied (6–10). The ϕ_2' coefficient, which reflects the binding of acetaldehyde to the enzyme-NADH complex, is related to the kinetic rate constants in Figure 4, as shown in Equation 1.

$$\phi'_2 = \frac{1}{k'_2}\left[1 + \frac{k'_{-2}}{k'}(1 + \frac{k}{k_{-2}})\right] \qquad \text{(Eq. 1)}$$

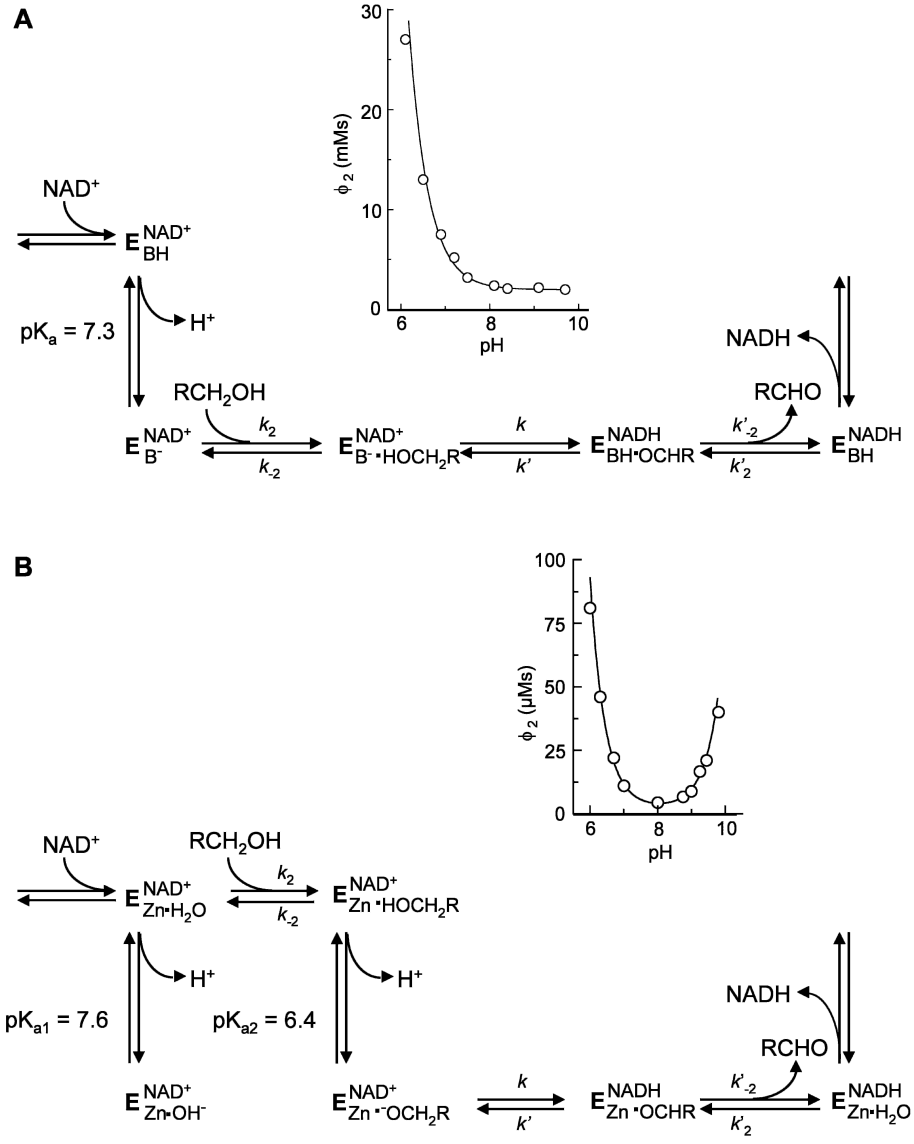

Figure 4. Mechanism proposed for *Drosophila* (*A*) and horse liver (*B*) ADH catalysis. (*A*) E denotes the enzyme and BH represents an ionizing group with a pK_a value of 7.1 and 7.3 in *D. lebanonensis* ADH at 23.5 and 19.0 °C respectively [49,50], and 7.6 in *D. melanogaster* ADH^S at 23.5 °C [47,64]. The panel inserted shows the variation of Φ_2 with varying pH for *D. lebanonensis* ADH at 19.0 °C, where $\Phi_2 = (1/k_2)(1+(k_{-2}/k)(1+(k'/k'_{-2})))$ and the kinetic constants are those shown in the compulsory ordered pathway. Only k_2, i.e. the k_{on} velocity for the alcohol varied with pH, and hence $\Phi_2 = \Phi^*_2\ (1+([H^+]/K_a))$. The theoretical curve is based on a pK_a of 7.3 and an Φ^*_2 of 2.0 mM. (*B*) The unified reaction mechanism for the oxidation of alcohols by HLADH as described by Kvassmann and Pettersson using benzyl alcohol [83], where $\Phi_2 = \Phi^*_2\ (1+([H^+]/(app)K_{a2}))^*(1+(K_{a1}/[H^+]))$. The theoretical curve is based on a Φ^*_2 of 0.286 μMs, a pK_{a1} of 7.6 and an (app)K_{a2} of 8.5 where the latter value is due to the k_{-2}/k quotient as follows; (app)$K_{a2} = K_{a2}{}^*(k^*_{-2}/k^*)$ and pK_{a2} is 6.4 and k^*_{-2}/k^* is $10^{-2.1}$.

This shows that k'_2 and the two quotients k'_{-2}/k' and k/k_{-2} were pH-independent, and hence there are no ionizable groups of catalytic importance within the pH region 6–10 in the ternary enzyme-NAD^+-alcohol and binary enzyme-NADH complexes. The two rate constants k'_{-2} and k', which reflect the ionization properties of the enzyme-NADH-acetaldehyde complex, must either show the same pH dependence or be pH-independent.

Binding of alcohol to the enzyme-NAD^+ complex is determined by the kinetic coefficient ϕ_2'. The variation of this coefficient with pH for the tested alcohols with both DADHs was dependent on the ionization of a single residue, as shown in Figure 4A. As discussed above, the absence of $[H^+]$ proportionality indicates that the pH dependence of the alcohol binding to the binary enzyme-NAD^+ complex is derived exclusively from the on-velocity constant. Further, the pH variation with pyrazole and 2,2,2-trifluoroethanol reveals that there is no drastic stickiness of the substrate. Therefore, the values obtained from the variation with pH for the two enzymes reflect the true pK_a value of a single residue (or two coupled residues that together lose one proton) in the binary enzyme-NAD^+ complex. Thus, a catalytic proton release occurs upon formation of the binary enzyme-NAD^+ complex (Fig. 4A). Also notable, there are no protons released upon formation of the ternary enzyme-coenzyme-substrate complexes or the binary enzyme-NADH complex. The proton release from the binary enzyme-NAD^+ complex is essential for alcohol binding and catalysis, as well as for binding of alcohol competitive inhibitors. The pH dependence of alcohol binding to the DADH-NAD^+ complex is different

from the corresponding pH dependence of the alcohol binding to the HLADH-NAD^+ complex, as shown in Figures 4A and B, and the cause of this difference is discussed below.

However, it is still not fully clear which amino acid in DADH is responsible for the catalytic proton release when NAD^+ binds and forms the binary enzyme-NAD^+ complex. Various amino acids have been suggested to be responsible for this catalytic proton release. Here we will give a short historical description of the various views. As sequencing studies show that Tyr151 and Lys155 are invariant within the SDR family [65], it was early suggested that Tyr151 or Lys155 could be responsible for the proton release [47]. However, comparison of the reaction mechanism of DADH with that of horse liver ADH showed that the proton release produced a negative charge at the active site and that something in this site had to act as a strong base or nucleophile to capture a proton from the bound substrate alcohol. Since site-directed mutagenesis studies showed that the two cysteine residues in DADH were of no catalytical importance [66] and along with newer available evidence of conserved residues in the SDR family [67–69], Tyr151 was then considered as the most likely candidate for this general base role [64]. Site-directed mutagenesis studies of DADH also demonstrated that both Tyr151 and Lys155 were essential for the enzymatic activity [70, 71]. When x-ray crystallographic data appeared for various SDR enzymes, including DADH [30, 34], it was shown that the hydroxyl groups of the inhibitors and substrate analogs in the ternary complexes were located between the hydroxyl groups of Tyr151 and Ser138. The hydroxyl group of Tyr151 is also in hydrogen-bonding distance to the O2′ hydroxyl group of the NAD^+-ribosyl moiety, and Lys155 is close to both the NAD^+-ribosyl O2′ and O3′ hydroxyl groups. Site-directed mutagenesis studies of Ser138 in several SDR enzymes, including DADH, have shown that this residue is also essential for the enzymatic activity [72]. The high ionization enthalpy of the pK_a value in DADH suggested that the proton-releasing group could not be the tyrosine (Tyr151), and it was instead concluded that the observed pH dependence could reflect the ionization of Ser138 [49, 50]. However, such a scenario requires that the pK_a value of Tyr151 is down-perturbed (<6) already in the binary E-NAD^+ complex, and hence not detectable in the kinetic studies where the pH varied from 6 to 10. However, kinetic studies of other SDR enzymes have further emphasized the hypothesis that the conserved Tyr151 acts as a general base during catalysis [73, 74]. A recent study using automatic docking of alcohol-competitive inhibitors to the binary DADH-NAD^+ complex, molecular dynamic simulations, and free-energy calculations indicates that the ionizing group is indeed Tyr151 [75]. A study based on theoretical calculations of possible ionizable groups in the binary DADH-NAD^+ complex suggests that it is neither the Ser138 nor Tyr151 that ionizes and regulates the binding of alcohols and alcohol-competitive inhibitors, but a coupled ionization of Tyr151 and Lys155 [76], as discussed in detail in the following paragraphs.

Theoretical evidence for a proton-relay mechanism in the catalysis of *Drosophila* alcohol dehydrogenase

In order to further characterize the active site of DADH, the ionization properties of the active-site residues in *Drosophila lebanonensis* alcohol dehydrogenase complexed with NAD^+ were investigated theoretically on the basis of a continuum dielectric model by using an approach developed to account for multiple locations of the hydrogen atoms of the titratable and polar groups [76–78]. Due to the inherent ambiguity of the available experimental data so far, the catalytic reaction mechanism can be explained by at least three models, named according to the group that loses its proton in the binary enzyme-NAD^+ complex and acts as a general base in the ternary enzyme-NAD^+-alcohol complex: the tyrosine-, lysine-, or serine mechanisms [33]. In order to promote hydride transfer from the substrate to the NAD^+ molecule during the oxidation reaction, one residue of the catalytic triad (the ionizing group that shows a pK_a of 7.6 in the binary *D. melanogaster* ADH-NAD^+ complex [49], Fig. 4) needs to abstract a proton from the Cα hydroxyl group of the substrate to generate an alcoholate anion. As mentioned in the previous section, it appears likely that Tyr151 is responsible for this pH behavior and acts as a general base during the reaction mechanism [30, 72, 79, 80]. However, theoretical calculations have resulted in a slightly modified view.

Theoretically calculated ionization properties of the active site residues

For Ser138, theoretical calculations indicate that Ser138 does not undergo deprotonation within the interval $2 < pH < 12$. The most populated rotamer of the hydroxyl group is that with a hydrogen bond between Wat144 (the active site bound water, see Fig. 5A) and the Ser138 hydroxyl group, in which the latter is the proton donor.

For Tyr151, the preferred state is to be protonated and act as a proton donor to the O2′ hydroxyl group of the NAD^+ ribose. The calculations show that the titration of Tyr151 displays two peculiarities: its ionization

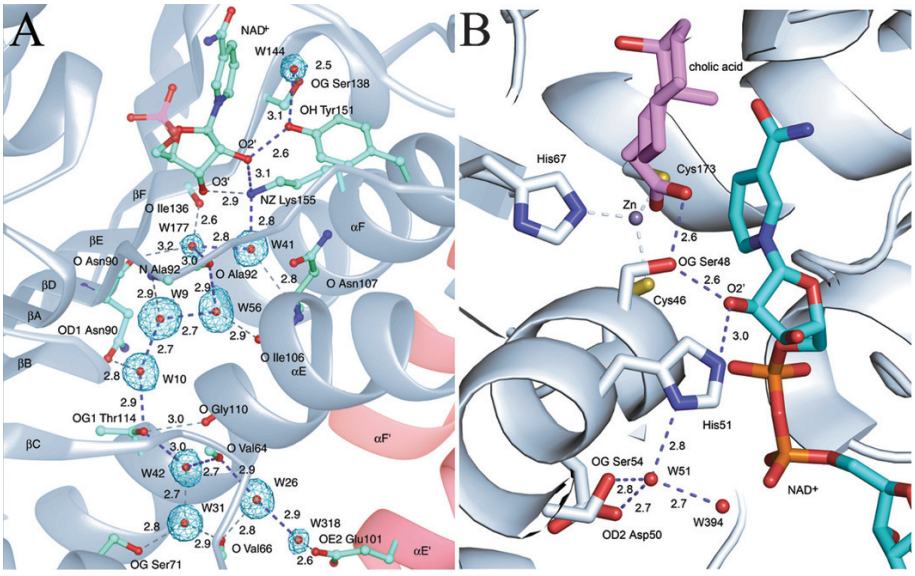

Figure 5. Water channels in ADHs. (*A*) The proton-relay chain in the *holo* form (NAD^+) of *Drosophila lebanonensis* ADH. The $2F_o$-F_c map is contoured at 1σ from the partially refined model (R value = 19% and free R value = 22%). The ribbon diagram is color-coded, depending on the subunit (B: pale blue; A: pale red). Oxygen, nitrogen, carbon, and phosphorus atoms are colored in red, blue, green, and magenta, respectively. Distances (Å) are shown as two types of dashed lines: dashed blue lines correspond to the hydrogen-bond proton-relay path that spans from the position of the alcohol substrate (its OH group is mimicked by Wat144; upper side of the figure) to water molecules exposed to the bulk solvent (Wat26 and Wat318; lower side of the figure). Dashed gray lines show hydrogen bond interactions between side-chain and backbone atoms and the members of the water channel. This picture was created with RIBBONS [114]. (*B*) The proton-relay chain in the *holo* form (NAD^+) of horse liver ADH. Oxygens, nitrogen, sulphurs, and phosphorus atoms are colored in red, blue, yellow, orange, respectively, and carbon atoms are either in cyan (NAD^+) or magenta (cholic acid). The distances are shown in Å as dashed lines: dashed blue lines correspond to the hydrogen-bond proton-relay path that spans from the alcohol substrate position (represented by the carboxylic group of the cholic acid; upper side of the figure) to water molecules exposed to the bulk solvent (Wat51 or Wat394; lower side of the figure); dashed light-gray lines show interactions between the Zn atom and its coordinating residues. This picture was created with PYMOL [111].

behavior in the two subunits differs at pH > 6 in one subunit and at pH > 10 in the other subunit of the dimer, and Tyr151 is partially deprotonated in the whole pH range.

For Lys155, the ionization behavior displays properties similar to those of Tyr151.

The ionization properties of Tyr151 and Lys155 in both subunits show an irregular titration curve that cannot be described by a typical Henderson–Hasselbalch equation [12, 21, 36, 78, 81].

pH dependence of the hydrogen atom populations in the active site hydrogen bond network

The calculations also show that the water molecule in the active site of the *holo* form of the enzyme (Wat144, Fig. 5A) preferably acts as a proton donor in the hydrogen bond with the Tyr151 hydroxyl group and as a proton acceptor with Ser138 (Fig. 5A).

The computations also reveal a strong pH dependence of the orientation of the hydrogen atom from the NAD^+ ribose O2′ hydroxyl group. At pH < 6, the NAD^+ ribose O2′ hydroxyl group is a proton acceptor in the hydrogen bond to Tyr151. The orientation at which the hydroxyl hydrogen is distant from both hydrogen bond partners is most populated. Accordingly, Tyr151 is preferably proton donor to the ribose hydroxyl (population 0.75) and proton acceptor in the hydrogen bond with Wat144. With increasing pH, the distribution of the ribose hydroxyl rotamers changes, and at neutral pH, all three states are approximately equally protonated. In this way, one can consider the hydroxyl group as freely rotating, so that it can serve as proton donor or acceptor to one or to the two hydrogen bond partners. At pH > 8, this distribution is reduced to a population of two states, at which the ribose hydroxyl is a proton donor/acceptor to Lys155 and Tyr151 with equal probability. The two hydrogen bond partners are also half-protonated.

pH dependence of the catalytic group in the binary DADH-NAD^+ complex

According to the electrostatic calculations, the population of the rotamer of Ser138 at which this residue is a proton acceptor is low, between 0.1 and 0.2. For this reason, Ser138 is most likely not responsible for the observed pH dependence and thus probably does not serve as a general base during the catalytic reaction. As mentioned above, the ionization of Tyr151 and Lys155 can be considered as a single ionization event. The fit to the Henderson–Hassel-

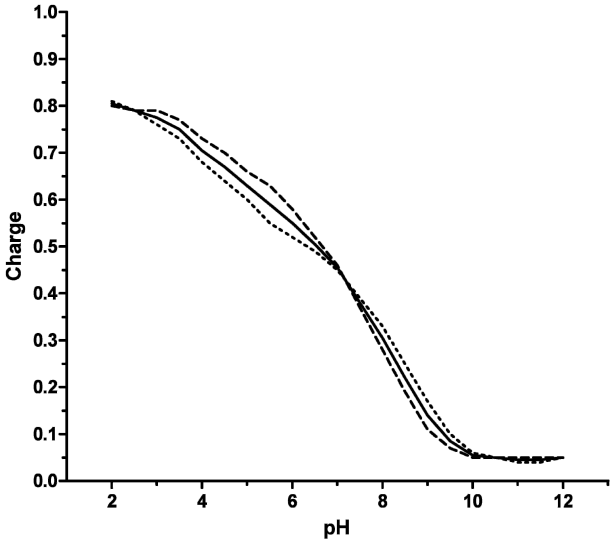

Figure 6. Calculated titration curve of the pair tyr151-lys155, showing coupled ionization: average over subunits A and B (solid line), subunit A (dashed line), subunit B (dotted line).

balch equation gives an apparent pK_a value of 7.2 for the curve averaged over the subunits A and B (Fig. 6). This value is in very good agreement with the experimental observations for *D. lebanonensis* ADH, which give a value between 7.1 and 7.3 [49, 50] (Fig. 4A).

A proton relay model of alcohol dehydrogenase activity in DADH

The preferred protonated state of the side chain of Tyr151 is to act as proton donor to the O2′ ribose OH group, which with equal probability has its OH proton towards both the Tyr151 and Lys155 side chains. Thus, after proton abstraction from the alcohol-substrate and protonation of Tyr151, the proton can be transported from the Tyr151 OH via the NAD^+-ribose OH to the amino group of Lys155. The calculations show that Lys155 is also half-protonated, in a manner that a proton donated by the NAD^+ ribose OH group can be accepted and released from the active site with equal probability (Fig. 7B). In this manner, the OH of Tyr151, the O2′ ribose OH , and the Lys155 ε-amino groups form a proton-relay chain (Fig. 7B, D). A key participant of the reaction mechanism of DADH is the NAD^+ ribosyl OH group, a OH group that functions as a *switch* in the proton-relay chain and is regulated by the protonation/deprotonation equilibrium of the coupled Tyr151/Lys155 ionization pair.

An eight-membered water chain connects the buried active site with the bulk solvent

Although Lys155 is buried in the protein during enzymatic catalysis, its ε-amino group is surrounded by a hydrophilic environment. In addition to the two OH groups of the NAD^+ ribose, Lys155 is hydrogen-bonded to a well-ordered water molecule (Wat41) (Fig. 5A). This water molecule is locked into position via hydrogen-bond interactions to the main chain of Asn107 and further connected to a water channel inside the protein fold (Wat177, Ala92-O, Wat56, Wat9, Wat10, Thr114-Oγ1, Wat42, Val64-O, Wat26, and Wat318), which connects Lys155 to the solvent space (Figure 5A).

The side chain of Asn107 forms two hydrogen-bond interactions with the main chain of Ile94, forcing the main chain of Asn107 to point away from the typical α-helical hydrogen-bond distribution and creating a hydrophilic environment inside the protein core and in the vicinity of Lys155. This interaction also results in a bend in the long α-helix E (Fig. 1A) that has been observed in most of all SDR structures available so far, suggesting that Asn107 is the fourth member of a catalytic tetrad instead of the initially proposed catalytic triad [82], since it is involved in the formation of this hydrophilic cavity, which seems important in catalysis.

These water molecules in the core of the protein are found in a distinct channel [30], where they are stabilized by hydrogen bonds to both backbone and side-chain atoms of the residues lining the channel (Fig. 5A). The last water molecule within the water chain (Wat318) is partially solvent-exposed and forms a hydrogen bond (2.6 Å) with Glu101 of the other subunit of the dimer. This water channel can be divided in two regions that are separated by Thr114, which links the inner and the outer segments of this water channel. The orientation of the hydrogen in the OH group of Thr114 shows a pH dependence that is similar to that of the NAD^+ ribose OH, i.e. it acts as an OH switch.

Thr114 together with all the other residues that form the water channel (Glu110, Tyr62, Asn90, Gly110, and Asn113) are invariant in all alcohol dehydrogenases from 119 *Drosophila* ADH sequences examined, pointing to their structural importance in DADH. All these water molecules are present in both binary and ternary complexes, which were obtained in diverse crystallization and temperature conditions, of two *Drosophila* species (*D. lebanonensis* and *D. melanogaster*) [30, 34] (Table 2).

Hypotheses on pH dependence for alcohol binding and proton translocation via the eight-membered water chain

Hypothesis 1

Based on the discovery of the eight-membered water chain in DADH, Koumanov et al. [76] provided the following interpretation for the proton release in the

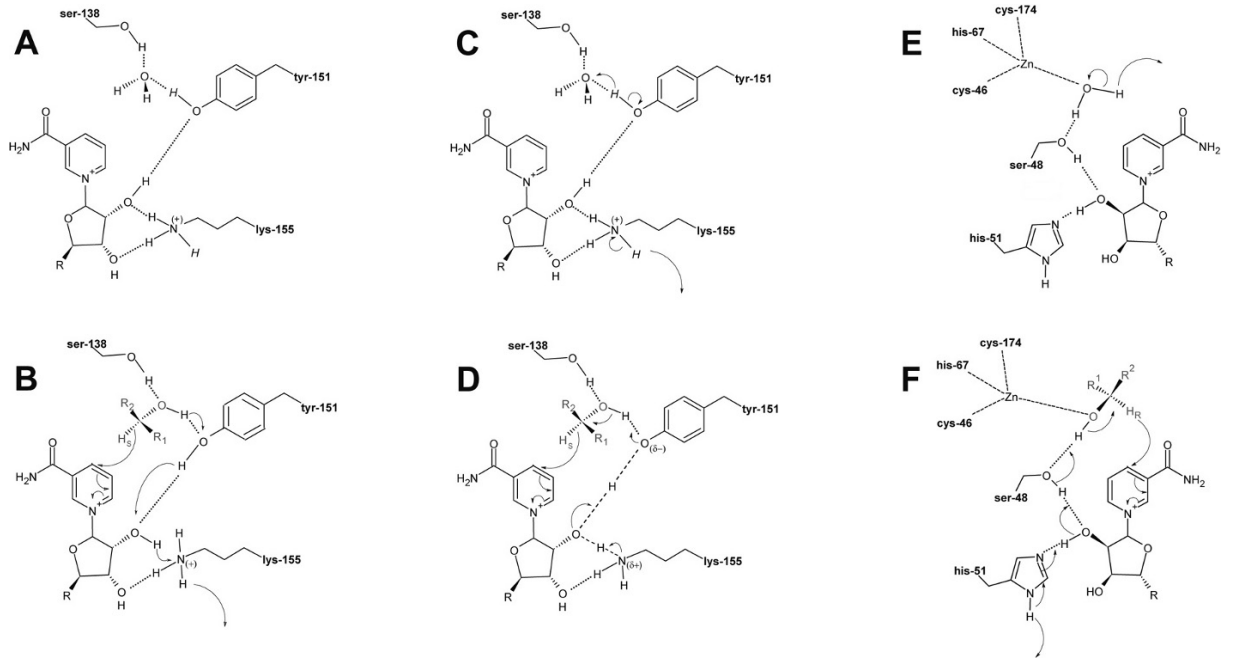

Figure 7. The proposed reaction mechanisms of DADH (*A* – *D*) and HLADH (*E*, *F*). A schematic representation of the binary and ternary DADH complexes, respectively, as described by hypothesis 1 (*A* and *B*) and hypothesis 2 (*C* and *D*). In the *holo* form of DADH with NAD^+ and a bound water molecule there is no ionization or proton release to the bulk solvent according to hypothesis 1 (*A*), while according to hypothesis 2 (*C*), the Tyr151/Lys155 couple acts as a single ionization group in this binary complex with a pK_a of ~ 7.2 (in Dl-ADH) or 7.6 (in Dm-ADHS). The proton release to the bulk solution is assumed to be partly through the water molecule in the active site and partly through the water channel as indicated by the arrows. (*B*) According to hypothesis 1, the Tyr151/Lys155 couple acts as a single ionization group in the ternary complex (with the above pK_a values) which abstracts the proton from the alcohol hydroxyl group and the proton is then released to the bulk solution through the water chain as indicated by the arrows. (*D*) In hypothesis 2, the proton at the alcohol hydroxyl group is abstracted to Tyr151 after the hydride transfer. As Tyr151/Lys155 is assumed to ionize as a single group, the proton of the alcohol is abstracted through a proton relay, but no proton is released to the bulk solvent as in hypothesis 1. The dashed line indicates that two protons are shared by three atoms, while the dotted lines indicate weak hydrogen bond interactions. The *holo* form of HLADH with NAD^+ and bound water molecule and where the bound water has a pK_a of ~ 7.6 (*E*) and the reaction mechanism of HLADH where the proton from the hydroxyl group of the alcohol is transferred to the solvent by Ser48, ribose O2′ group, and His51 (*F*). This figure was created with the free version of ACD/3D (Advanced Chemistry Development, Inc., Toronto, Ontario, Canada).

oxidation of alcohols. According to the calculations discussed above, substrate binding is pH independent (Fig. 7A). The proton abstracted from the hydroxyl group of the alcohol is taken out of the active site via the eight-membered water chain (Fig. 7B). Hence, the pH dependence for the oxidation of alcohols seen in Figure 4A is due to a pH dependence of the hydride transfer step (k) in the ternary complex where the obtained pK_a value is an apparent value derived from the $[H^+]$ proportionality of the quotients k_{-2}/k in a way similar to that indicated for the proton release of the alcohol in the ternary complex of HLADH (Fig. 4B) [75]. The main difference between DADH and HLADH based on this hypothesis is the lack of a proton release in the binary DADH-NAD^+ complex (Fig. 7A), while in the binary HLADH-NAD^+ complex a non-catalytic proton release occurs from the zinc-bound water to the solvent (Figs. 4B, 7E).

Hypothesis 2

This hypothesis is based on the interpretation of McKinley–McKee et al. [64] and Winberg et al. [49, 50], along with the new theoretical calculations by Koumanov et al. [76]. In this scenario, the pH dependency for the binding of alcohols (Fig. 4A) and alcohol competitive inhibitors to the DADH-NAD^+ is derived exclusively from a proton release from the binary DADH-NAD^+ complex, as discussed above. The proton fraction released from the NH_3-group of Lys155 will be transported to the solvent through an eight-membered water chain, while the fraction released from the OH group of Tyr151 goes directly to the water in the active site (Fig. 7C). A proton release involving a coupled ionization of Tyr151 and Lys155 may explain the high value for the ionization enthalpy of the pK_a with ethanol and pyrazole. In this model, the proton abstracted from the hydroxyl group of the alcohol is taken up by the partly negatively charged oxygen at Tyr151 (Fig. 7D), and no proton release to the solvent occurs at the ternary complex

level. The essential difference between the pH dependence of DADH in this model and HLADH is that in the HLADH enzyme, the catalytic proton release occurs in the ternary enzyme-NAD^+-alcohol complex forming an enzyme-NAD^+-alcoholate complex (Figs. 4B, 7F) [64, 83], while in DADH the catalytic proton release occurs at the binary enzyme-NAD^+ level (Figs. 4A, 7C). Another aspect that may differ between the two enzymes is the stage in the mechanism where the proton release from the bound alcohol occurs. In HLADH, the release occurs prior to the hydride transfer step and hence facilitates this step (Fig. 4B). Although a similar explanation for the oxidation of alcohols with DADH has been proposed [64], it is a problem to envisage how a group with $pK_a \sim 7.6$ (Tyr151 in the Dm-ADH^S-NAD^+ complex), which is half-protonated at physiological pH of ~7.6, can abstract a proton from an alcohol which usually shows a pK_a of around 16. Therefore it appears more probable that with DADH, the proton release from the bound alcohol to the ionized Tyr151 occurs after the hydride transfer step. The formed NADH perturbs the pK_a of the Tyr151/Lys 155 couple to a higher value, and hence is able to abstract the loosely bound proton on the formed aldehyde/ketone. Such a mechanism will also explain the release of a proton from Tyr151 to the aldehyde in the reverse reaction. Thus, the mechanism for proton release in the non-metallo enzyme DADH appears to be distinctly different from that in the zinc-containing HLADH.

Comparison of DADH and HLADH pH dependence

The zinc-containing horse liver ADH also operates in a compulsory ordered ternary-complex mechanism with coenzyme as the leading substrate [58, 59, 84–86]. This enzyme responds to pH changes similarly to DADH [83, 86–89], as coenzyme and alcohol binding are strongly influenced, whereas the binding of aldehyde substrates remains unaffected. As in DADH, a proton is released upon binding of NAD^+ to HLADH. This proton is assumed to come from the zinc-bound water (Figs. 4B, 7E). However, the release of this proton represents a side reaction that is not on the catalytic pathway [83]. In the HLADH enzyme, a catalytic proton release to the solvent occurs in the ternary enzyme-NAD^+-alcohol complex forming an enzyme-NAD^+-alcoholate complex (Fig. 7F) [64, 83]. X-ray crystallographic studies on HLADH show that the proton released from the bound alcohol in the ternary complex cannot be directly transferred to solution [62, 90] instead, the proton is shuttled through a proton-relay system involving Ser48 (Figs. 5B, 7F), the hydroxyl group from the nicotinamide ribose group of the NAD^+ and His51 [90–92]. Site-directed mutagenesis of His51 in HLADH suggests that it participates, although not essentially, during proton transfer in the reaction mechanism [93]. Thus, both DADH and HLADH contain a buried water channel that may participate in a proton-relay system.

ADH activity among different fruit-fly species

Transition-state theory relates the free activation energy $\Delta G^{\neq}$ and the first-order rate constant k_1 (Eqs. 2 and 3):

$$\ln k_1 = \ln\left(\frac{kT}{h}\right) - \Delta H^{\neq}/RT + \Delta S^{\neq}/RT \qquad \text{(Eq. 2)}$$

$$k_1 = \left(\frac{kT}{h}\right)e^{-\Delta G^{\neq}} = \left(\frac{kT}{h}\right)e^{-\Delta H^{\neq}/RT}e^{\Delta S^{\neq}/R} \qquad \text{(Eq. 3)}$$

The plot ln k_1 versus the calculated electric field $\Delta H^{\neq}$ shows an almost linear relationship (Eq. 2) for all the alleloforms examined when using the theoretically calculated electrostatic field $\Delta H^{\neq}$ and the values of experimentally obtained k_{cat} of propan-2-ol [32, 35]. For this alcohol, the rate-limiting step is the release of the twice negatively charged coenzyme molecule (NADH). The more negative the active site is, the faster it will be to release NADH and the faster the total reaction will be, if the release of NADH is the rate-limiting step. The different alleloforms differ by just a few residues that alter the total electrostatic field at the active site (Table 1) [35]. Dm-ADH^S, a slower enzyme, has a more positively charged active site than the faster Dm-ADH^{UF} [35] (Table 1). This seems to suggest that the turnover is altered by changes solely in the electrostatic properties of the active site of the enzyme and not by conformational changes. Since sequence differences involving charged residues on the surface account for one-third of all the substitutions among DADHs, it appears that to some extent electrostatic interactions between the coenzyme and the enzyme are the main factor that affects the efficiency of the enzymatic reaction. It would seem that the effects of core-residue substitutions among different *Drosophila* ADHs are finely tuned to preserve the overall fold of the enzyme, and as a result maintain the substrate/coenzyme binding conformation.

It should be possible to comparatively predict the catalytic efficiency of many DADHs based only on their primary structure and a reasonably-built 3D model from Dm-ADH^S or any other available DADH coordinates (Table 2). The predicted enzymatic behavior for several DADHs belonging to the group *melanogaster* were estimated theoretically (k_{cat} value for propan-2-ol) [32]. These results predict that *D.*

tsacasi ADH and *D. yakuba* ADH should have a k_{cat} value that is lower than that of *D. simulans* ADH or Dm-ADH^{S} (Table 1). Furthermore, *D. erecta* ADH should have a k_{cat} value close to that of Dm-ADH^{F}. DADHs belonging to other *Drosophila* subgenus have also been modeled [32] by consideration of a representative of each group and calculation of the theoretical k_{cat}. These considerations predict that *D. hydey1* ADH should have a k_{cat} value higher than that of Dm-ADH^{UF}, followed by *D. crassifemur* ADH and *D. affinidisjunta* ADH, results that need to be experimentally cross-examined.

It would seem as if at this level of speciation, the mechanism by which evolution has chosen to tweak the activity of an enzyme is by modifying the electrostatic field around the active site and ignoring or canceling out other sequence substitutions to preserve the overall fold and binding environment of the rate-limiting substrate (in the case of secondary alcohols, the release of NADH).

Concluding remarks and future directions

The determination of the crystal structure of the short-chain ADH from *Drosophila* represented an inflection point in understanding this metal-free ADH. The crystal structure was able to further understand a myriad of mutagenesis and kinetic studies that preceded the three-dimensional structure determination, studies that were only partly understood until the 3D structure was unveiled. The vast biochemical information gathered throughout the years and the seven high-resolution structure entries available in the PDB represent a situation that is unique among the SDR enzymes. Therefore, this enzyme can be the cornerstone of new studies that deal with the complicated structure-function mechanisms of evolutionary fitness at the molecular level.

Although several studies have been carried out that describe the pH dependence of the kinetic coefficients of DADH and other SDRs, none of these studies have been able to directly show which residue(s) in the active site becomes partly or fully deprotonated upon formation of the enzyme-NAD(P)$^{+}$ complex and is responsible for abstraction of a proton from the alcohol substrate. Future work is needed in order to fully explain the exact function of the water channel in DADH and SDRs and if their proton-relay system is indeed involved in capturing the proton lost during the formation of the enzyme-NAD^{+} complex. Some of these studies could be classical inactivation kinetics linked to mass spectroscopy studies, site-directed mutagenesis of critical residues that create the water channel, along with x-ray crystallographic studies, and enzyme kinetics.

Since DADH appears to crystallize easily and high-resolution structures to up to 1.1-Å resolution have been obtained with reasonable facility (Table 2), it should be possible to perform proton titration of selected residues of the *holo* or ternary forms of the enzyme in crystalline form. This could be accomplished by measurement of the crystal structure at atomic resolution (x-ray diffraction better than 1 Å) or by neutron diffraction experiments at different pHs and observing the occupancy of the respective protons as pH changes [94].

The conversion of the biologically important DADH-5 to DADH-3 and DADH-1 by NAD^{+} and ketones is also not fully understood. Although isolation of the conversion factor from the DADH-1 form has shown that an NAD^{+}-ketone adduct is reversibly bound to the enzyme, more detailed kinetic studies on the conversion from one enzyme form to the other are needed. Such studies should also include the pH dependence of the conversion process. More detailed studies of the conversion process will give us more information on the structure-function properties of the active site in DADH, as the conversion process actually occurs due to the formation of a product inhibitory complex of importance to the life cycle of the fly.

Although crystallography tends to show us a static view of proteins, proteins as large polymers are anything but static. Proton shuffling, concerted movements, side-chain conformational fluctuations, and quantum mechanical considerations must be treated before we can understand how a reaction actually works at the active site of the enzyme. With the advent of computer power available nowadays, it should be possible to perform hybrid quantum mechanical/molecular modeling (QM/MM) calculations to simulate the active site of DADH and to give us newer insight into its reaction mechanism. The amount of crystallographic and kinetic data gathered so far, especially the 1.1-Å resolution structure of the complex of *D. lebanonensis* ADH with NAD^{+} and 2,2,2-trifluoroethanol, should give us a good head start for these kind of calculations (Table 2).

Recently, concerted atomic motions within the enzyme seem to correlate with its activity. Solution NMR relaxation experiments could identify residues that are important to the protein internal motions [95]. These studies could give a correlation between distant replacements in the protein and their effects on the enzymatic activity, or explain the acquired thermostability of the enzyme with just a couple of sequence replacements in Dm-ADH^{FCh} (Table 1), or even the

preference for a dehydrogenase rather than a reductase assignment.

It would also be of interest to understand whether electrostatic differences are the only factor in tweaking the enzymatic activity of ADHs from different *Drosophila* species. To understand this, determination of k_{cat} values of several DADHs and their crystal structure would be needed. This can tell us whether surface changes among DADH are the sole factor responsible for fine-tuning the efficiency of the enzyme or whether there are other mechanisms involved. This could indeed unite the speciacion of thousands of *Drosophila* species spread throughout the planet with the three-dimensional structure of the enzyme and may explain similar phenomena in other SDR enzymes or speciation systems. Furthermore, due to the sequence similarity of ADHs from other *Drosophila* species, it is expected that crystallization conditions may be very similar to the already published ones [30, 32, 34].

Finally, although we are quite proficient about the origins and evolution of new genes by gene duplication, and exon shuffling [96], the generation of new functions under positive Darwinian selection remains an interesting problem. Recently, Zhang et al. [97] examined a newly evolved gene that results in a protein called Jingwei that arose only 2.5 million years ago in *D. yakuba* and *D. teissieri*, two African *Drosophila* species, a gene that is very similar to that of DADH but that has a number of interesting characteristics. New structural, kinetic, and genetic data on these new genes would also be of interest to understand why some amino acid replacements outside active sites result in unexpected functional changes in a new gene [97].

1 Danielsson, O., Atrian, S., Luque, T., Hjelmqvist, L., Gonzàlez-Duarte, R. and Jörnvall, H. (1994). Fundamental molecular differences between alcohol dehydrogenase classes. Proc. Natl. Acad. Sci. USA 91, 4980–4984.

2 Jörnvall, H., Nordling, E. and Persson, B. (2003). Multiplicity of eukaryotic ADH and other MDR forms. Chemico-Biological Interactions 143–144, 255–261.

3 Manchester, S. R. and Kress, W. J. (1993). Fossil bananas (Musaceae): *Ensete oregonense* sp. nov. from the Eocene of western North America and its phytogeographic significance. Am. J. Bot. 80, 1264–1272.

4 Schilthuizen, M. (2000). Dualism and conflicts in understanding speciation. Bioessays 22, 1134–1141.

5 Persson, B., Krook, M. and Jörnvall, H. (1991). Characteristics of short-chain alcohol dehydrogenases and related enzymes. Eur. J. Biochem. 200, 537–543.

6 Kallberg, Y., Oppermann, U., Jörnvall, H. and Persson, B. (2002). Short-chain dehydrogenase/reductase (SDR) relationships: a large family with eight clusters common to human, animal, and plant genomes. Protein Sci. 11, 636–641.

7 Kallberg, Y., Oppermann, U., Jörnvall, H. and Persson, B. (2002). Short-chain dehydrogenases/reductases (SDRs). Eur. J. Biochem. 269, 4409–17.

8 Oppermann, U., Filling, C., Hult, M., Shafqat, N., Wu, X., Lindh, M., Shafqat, J., Nordling, E., Kallberg, Y., Persson, B. et al. (2003). Short-chain dehydrogenases/reductases (SDR): the 2002 update. Chem. Biol. Interact. 143–144, 247–253.

9 Gasteiger, E., Gattiker, A., Hoogland, C., Ivanyi, I., Appel, R. D. and Bairoch, A. (2003). ExPASy: the proteomics server for in-depth protein knowledge and analysis. Nucleic Acids Res. 31, 3784–3788.

10 Gramser, S. (2005). Alcohol and science: the party gene. Nature 438, 1068–1069.

11 Ashburner, M. (1998). Speculations on the subject of alcohol dehydrogenase and its properties in *Drosophila* and other flies. Bioessays 20, 949–954.

12 Umina, P. A., Weeks, A. R., Kearney, M. R., McKechnie, S. W. and Hoffmann, A. A. (2005). A rapid shift in a classic clinal pattern in Drosophila reflecting climate change. Science 308, 691–693.

13 Benyajati, C., Place, A. R., Powers, D. A. and Sofer, W. (1981). Alcohol dehydrogenase gene of *Drosophila melanogaster*: relationship of intervening sequences to functional domains in the protein. Proc. Natl. Acad. Sci. USA 78, 2717–2721.

14 Schwartz, M., O'Donnell, J. and Sofer, W. (1979). Origin of the multiple forms of alcohol dehydrogenase from Drosophila melanogaster. Arch. Biochem. Biophys. 194, 365–78.

15 Sofer, W. and Ursprung, H. (1968). *Drosophila* alcohol dehydrogenase. Purification and partial characterization. J. Biol. Chem. 243, 3110–3115.

16 Sofer, W. and Martin, P. F. (1987). Analysis of alcohol dehydrogenase gene expression in Drosophila. Annu. Rev. Genet. 21, 203–225.

17 Chambers, G. K. (1991). Gene expression, adaptation and evolution in higher organisms. Evidence from studies of *Drosophila* alcohol dehydrogenases. Comp. Biochem. Physiol. Sect. B 99, 723–730.

18 Winberg, J.-O. and McKinley-McKee, J. S. (1992). Kinetic interpretations of active site topologies and residue exchanges in *Drosophila* alcohol dehydrogenases. Int. J. Biochem. 24, 169–181.

19 Heinstra, P. W. (1993). Evolutionary genetics of the *Drosophila* alcohol dehydrogenase gene-enzyme system. Genetica 92, 1–22.

20 Guarnieri, D. J. and Heberlein, U. (2003). Drosophila melanogaster, a genetic model system for alcohol research. Int. Rev. Neurobiol. 54, 199–228.

21 Johnson, F. M. and Dennistone, C. (1964). Genetic variation of alcohol dehydrogenase in *Drosophila melanogaster*. Nature 204, 906–907.

22 Grell, E. H., Jacobson, K. B. and Murphy, J. B. (1965). Alcohol dehydrogenase in *Drosophila melanogaster*: isozymes and genetic variants. Science 149, 80–82.

23 Ursprung, H. and Leone, J. (1965). Alcohol dehydrogenase: a polymorphism in *Drosophila melanogaster*. J. Exp. Zool. 160, 147–154.

24 Goldberg, D. A. (1980). Isolation and partial characterization of the *Drosophila* alcohol dehydrogenase gene. Proc. Natl. Acad. Sci. USA 77, 5794–5798.

25 Freriksen, A., de Ruiter, B. L., Scharloo, W. and Heinstra, P. W. (1994). Drosophila alcohol dehydrogenase polymorphism and carbon-13 fluxes: opportunities for epistasis and natural selection. Genetics 137, 1071–1078.

26 Heinstra, P. W., Scharloo, W. and Thörig, G. E. W. (1986). Alcohol dehydrogenase of *Drosophila*: conversion and retroconversion of isozyme patterns. Comp. Biochem. Physiol. Sect. B 83, 409–414.

27 Anderson, S. M. and McDonald, J. F. (1981). Effect of environmental alcohol on *in vivo* properties of *Drosophila* alcohol dehydrogenase. Biochem. Genet. 19, 421–430.

28 Chenevert, S. W., Fosset, N. G., Chang, S. H., Tsigelny, I., Baker, M. E. and Lee, W. R. (1995). Amino acids important in enzyme activity and dimer stability for *Drosophila* alcohol dehydrogenase. Biochem. J. 308, 419–423.

29 Thatcher, D. R. (1980). The complete amino acid sequence of three alcohol dehydrogenase alleloenzymes (adh^{n-11}, adh^{s} and adh^{uf}) from the fruitfly *Drosophila melanogaster*. Biochem. J. 187, 875–883.

30 Benach, J., Atrian, S., Gonzàlez-Duarte, R. and Ladenstein, R. (1998). The refined crystal structure of *Drosophila lebanonensis* alcohol dehydrogenase at 1.9 Å resolution. J. Mol. Biol. 282, 383–399.

31 Ghosh, D., Weeks, C. M., Grochulski, P., Duax, W. L., Erman, M., Rimsay, R. L. and Orr, J. C. (1991). Three-dimensional structure of holo 3α,20β-hydroxysteroid dehydrogenase: a member of a short-chain dehydrogenase family. Proc. Natl. Acad. Sci. USA 88, 10064–10068.

32 Benach, J., Winberg, J. O., Svendsen, J. S., Atrian, S., Gonzalez-Duarte, R. and Ladenstein, R. (2005). *Drosophila* alcohol dehydrogenase: acetate-enzyme interactions and novel insights into the effects of electrostatics on catalysis. J. Mol. Biol. 345, 579–598.

33 Benach, J. (1999) X-ray structure analysis of short-chain dehydrogenases/reductases. Doctoral thesis, Karolinska Institute, Stockholm.

34 Benach, J., Atrian, S., Gonzàlez-Duarte, R. and Ladenstein, R. (1999). The catalytic reaction and inhibition mechanism of *Drosophila* alcohol dehydrogenase: observation of an enzyme-bound NAD-ketone adduct at 1.4 Å resolution by X-ray crystallography. J. Mol. Biol. 289, 335–355.

35 Benach, J., Atrian, S., Fibla, J., Gonzàlez-Duarte, R. and Ladenstein, R. (2000). Structure-function relationships in *Drosophila melanogaster* alcohol dehydrogenase allozymes ADH^{S}, ADH^{F} and ADH^{UF}, and distantly related forms. Eur. J. Biochem. 267, 3613–3620.

36 Holm, L. and Sander, C. (1993). Protein structure comparison by alignment of distance matrices. J. Mol. Biol. 233, 123–138.

37 Albalat, R., Valls, M., Fibla, J., Atrian, S. and Gonzàlez-Duarte, R. (1995). Involvement of the C-terminal tail in the activity of *Drosophila* alcohol dehydrogenase. Evaluation of truncated proteins constructed by site-directed mutagenesis. Eur. J. Biochem. 233, 498–505.

38 Chen, Z., Lee, W. R. and Chang, S. H. (1991). Role of aspartic acid 38 in the cofactor specificity of *Drosophila* alcohol dehydrogenase. Eur. J. Biochem. 202, 263–267.

39 Winberg, J.-O., Thatcher, D. R. and McKinley-McKee, J. S. (1982). Alcohol dehydrogenase from the fruitfly *Drosophila melanogaster* substrate specificity of the alleloenzymes Adh^{S} and Adh^{UF}. Biochim. Biophys. Acta 704, 7–16.

40 Hovik, R., Winberg, J.-O. and McKinley-McKee, J. S. (1984). *Drosophila melanogaster* alcohol dehydrogenase. Substrate stereospecificity of the Adh^{F} alleloenzyme. Insect Biochem. 14, 345–351.

41 Winberg, J.-O., Hovik, R., McKinley-McKee, J. S., Juan, E. and Gonzàlez-Duarte, R. (1986). Biochemical properties of alcohol dehydrogenase from *Drosophila lebanonensis*. Biochem. J. 235, 481–490.

42 Eisses, K. T., Davies, S. L. and Chambers, G. K. (1994). Substrate and inhibition studies of the thermostable alcohol dehydrogenase allozymes ADH-71k and ADH-FCh.D of *Drosophila*. Biochem. Genet. 32, 91–103.

43 Eisses, K. T. (1989). On the oxidation of aldehydes by alcohol dehydrogenase of *Drosophila melanogaster*: evidence for the gem-diol as the reacting substrate. Bioorg. Chem. 17, 268–274.

44 Henehan, G. T. M., Chang, S. H. and Oppenheimer, N. J. (1995). Aldehyde dehydrogenase-activity of *Drosophila melanogaster* alcohol dehydrogenase burst kinetics at high pH and aldehyde dismutase activity at physiological pH. *Biochemistry* 34, 12294–12301.

45 Winberg, J.-O. and McKinley-McKee, J. S. (1998). *Drosophila melanogaster* alcohol dehydrogenase: mechanism of aldehyde oxdiation and dismutation. Biochem. J. 329, 561–570.

46 Winberg, J.-O., Thatcher, D. R. and McKinley-McKee, J. S. (1982). Alcohol dehydrogenase from the fruitfly *Drosophila Melanogaster* inhibition studies of the alleloenzymes Adh^{S} and Adh^{UF}. Biochim. Biophys. Acta 704, 17–25.

47 Winberg, J.-O. and McKinley-McKee, J. S. (1988). The Adh^{s} alleloenzyme of alcohol dehydrogenase from *Drosophila melanogaster*. Variation of kinetic parameters with pH. Biochem. J. 255, 589–599.

48 Winberg, J.-O. and McKinley-McKee, J. S. (1994). *Drosophila melanogaster* alcohol dehydrogenase: product-inhibition studies. Biochem. J. 301, 901–909.

49 Brendskag, M. K., McKinley-McKee, J. S. and Winberg, J.-O. (1999). *Drosophila lebanonensis* alcohol dehydrogenase: pH dependence of the kinetic coefficients. Biochim. Biophys. Acta 1431, 74–86.

50 Winberg, J.-O., Brendskag, M. K., Sylte, I., Lindstad, R. I. and McKinley-McKee, J. S. (1999). The catalytic triad in *Drosophila* alcohol dehydrogenase: pH, temperature and molecular modelling studies. J. Mol. Biol. 294, 601–616.

51 Winberg, J.-O., Thatcher, D. R. and McKinley-McKee, J. S. (1983). *Drosophila melanogaster* Alcohol Dehydrogenase: an electrophoretic study of the Adh^{S}, Adh^{F} and Adh^{UF} alleloenzymes. Biochem. Genet. 21, 63–80.

52 Winberg, J.-O. and McKinley-McKee, J. S. (1988). *Drosophila melanogaster* alcohol dehydrogenase. Biochemical properties of the NAD^{+}-plus-acetone-induced isoenzyme conversion. Biochem. J. 251, 223–227.

53 Allemann, R. K., Hung, R. and Benner, S. (1988). Stereochemical profile of the dehydrogenases of *Drosophila melanogaster*. J. Am. Chem. Soc. 110, 5555–5560.

54 Winberg, J.-O., Martinoni, B., Roten, C. and McKinley-Mckee, J. S. (1993). *Drosophila* Alcohol dehydrogenase: stereoselective hydrogen transfer from ethanol. Biochem. Mol. Biol. Int. 31, 651–658.

55 Pilka, E. S., Guo, K., Kavanagh, K., Von Delft, F., Arrowsmith, C., Weigelt, J., Edwards, A., Sundstrom, M., Oppermann, U. and Structural Genomics Consortium (2006) Crystal structure of 15-hydroxyprostaglandin dehydrogenase type1, complexed with NAD+. Protein Data Bank. DOI: 10.2210/pdb2gdg/pdb.

56 MacKenzie, A., Kershaw, N., Hernandez, H., Robinson, C., Schofield, C. and Andersson, I. (2007). Clavulanic acid dehydrogenase: structural and biochemical analysis of the final step in the biosynthesis of the beta-lactamase inhibitor clavulanic acid. Biochemistry 1523–1533.

57 Benach, J., Atrian, S., Ladenstein, R. and Gonzalez-Duarte, R. (2001). Genesis of *Drosophila* ADH: the shaping of the enzymatic activity from a SDR ancestor. Chem. Biol. Interact. 130–132(1–3), 405–415.

58 Dalziel, K. and Dickinson, F. M. (1966). The kinetics and mechanism of liver alcohol dehydrogenase with primary and secondary alcohols as substrates. Biochem. J. 100, 34–46.

59 Tsai, C. S. (1968). Relative reactivities of primary alcohols as substrates of liver alcohol dehydrogenase. Can. J. Biochem. 46, 381–385.

60 Merritt, A. D. and Tomkins, G. M. (1959). Reversible oxidation of cyclic secondary alcohols by Liver Alcohol Dehydrogenase. J. Biol. Chem. 234, 2778–2782.

61 Dickinson, F. M. and Dalziel, K. (1967). Substrate specificity and stereospecificity of alcohol dehydrogenases. Nature 214, 31–33.

62 Eklund, H., Plapp, B. V., Samama, J. P. and Brändén, C. I. (1982). Binding of substrate in a ternary complex of horse liver alcohol dehydrogenase. J. Biol. Chem. 257, 14349–14358.

63 Reynier, M. and Theorell, H. (1969). Studies on the stereospecificity of liver alcohol dehydrogenase (LADH) for 3beta-hydroxy-5beta-steroids. Inhibition effect of pyrazole and of a 3alpha-hydroxycholanoic acid. Acta Chem. Scand. 23, 1130–1136.

64 McKinley-McKee, J., S., Winberg, J.-O. and Pettersson, G. (1991). Mechanism of action of *Drosophila* alcohol dehydrogenase. Biochem. Int. 25, 879–885.

65 Jörnvall, H., Persson, M. and Jeffery, J. (1981). Alcohol and polyol dehydrogenases are both divided into two protein types, and structural properties cross-relate the different enzyme activities within each type. Proc. Natl. Acad. Sci. USA 78, 4226–4230.
66 Chen, Z., Lu, L., Shirley, M., Lee, W. R. and Chang, S. H. (1990). Site-directed mutagenesis of glycine-14 and two 'critical' cysteinyl residues in *Drosophila* alcohol dehydrogenase. Biochemistry 29, 1112–1118.
67 Krook, M., Marekov, L. and Jörnvall, H. (1990). Purification and structural characterization of placental NAD(+)-linked 15-hydroxyprostaglandin dehydrogenase. The primary structure reveals the enzyme to belong to the short-chain alcohol dehydrogenase family. Biochemistry 29, 738–743.
68 Marekov, L., Krook, M. and Jörnvall, H. (1990). Prokaryotic 20 beta-hydroxysteroid dehydrogenase is an enzyme of the 'short-chain, non-metalloenzyme' alcohol dehydrogenase type. FEBS Lett. 266, 51–54.
69 Ensor, C. M. and Tai, H. H. (1991). Site-directed mutagenesis of the conserved tyrosine 151 of human placental NAD+-dependent 15-hydroxyprostaglandin dehydrogenase yields a catalytically inactive enzyme. Biochem. Biophys. Res. Commun. 30, 840–845.
70 Chen, Z., Jiang, J. C., Lin, Z.-G., Lee, W. R., Baker, M. E. and Chang, S. H. (1993). Site-specific mutagenesis of *Drosophila* alcohol dehydrogenase: evidence for involvement of Tyrosine-152 and Lysine-156 in catalysis. Biochemistry 32, 3342–3346.
71 Cols, N., Atrian, S., Benach, J., Ladenstein, R. and Gonzàlez-Duarte, R. (1997). Drosophila alcohol dehydrogenase: evaluation of Ser139 site-directed mutants. FEBS Lett. 413, 191–193.
72 Cols, N., Marfany, G., Atrian, S. and Gonzàlez-Duarte, R. (1993). Effect of site-directed mutagenesis on conserved positions of *Drosophila* alcohol dehydrogenase. FEBS Lett. 319, 90–94.
73 Gerratana, B., Cleland, W. W. and Frey, P. A. (2001). Mechanistic roles of Thr134, Tyr160, and Lys 164 in the reaction catalyzed by dTDP-glucose 4,6-dehydratase. Biochemistry 40, 9187–9195.
74 Hwang, C. C., Chang, Y. H., Hsu, C. N., Hsu, H. H., Li, C. W. and Pon, H. I. (2005). Mechanistic roles of Ser-114, Tyr-155, and Lys-159 in 3alpha-hydroxysteroid dehydrogenase/carbonyl reductase from Comamonas testosteroni. J. Biol. Chem. 280, 3522–3528.
75 Gani, O. A., Adekoya, O. A., Giurato, L., Spyrakis, F., Cozzini, P., Guccione, S., Winberg, J. O. and Sylte, I. (2008). Theoretical calculatons of the catalytic triad in short chain alcohol dehydrogenases/reductases. Biophys. J. 94, 1412–1427.
76 Koumanov, A., Benach, J., Atrian, S., Gonzalez-Duarte, R., Karshikoff, A. and Ladenstein, R. (2003). The catalytic mechanism of *Drosophila* alcohol dehydrogenase: evidence for a proton relay modulated by the coupled ionization of the active site Lysine/Tyrosine pair and a NAD^+ ribose OH switch. Proteins 51, 289–298.
77 Bashford, D. and Karplus, M. (1990). pKa's of ionizable groups in proteins: atomic detail from a continuum electrostatic model. Biochemistry 29, 10219–10225.
78 Koumanov, A., Rueterjans, H. and Karshikoff, A. (2002). Continuum electrostatic analysis of irregular ionization and proton allocation in proteins. Proteins 46, 85–96.
79 Ghosh, D., Wawrzak, Z., Weeks, C. M., Duax, W. L. and Erman, M. (1994). The refined three-dimensional structure of 3α,20β-hydroxysteroid dehydrogenase and possible roles of the residues conserved in short-chain dehydrogenases. Structure 2, 629–640.
80 Tanaka, N., Nonaka, T., Tanabe, T., Yoshimoto, T., Tsuru, D. and Mitsui, Y. (1996). Crystal structures of the binary and ternary complexes of 7α-hydroxysteroid dehydrogenase from *Escherichia coli*. Biochemistry 35, 7715–7730.
81 Bashford, D. and Gerwert, K. (1992). Electrostatic calculations of the pKa values of ionizable groups in bacteriorhodopsin. . J. Mol. Biol. 224, 473–486.
82 Filling, C., Berndt, K. D., Benach, J., Knapp, S., Prozorovski, T., Nordling, E., Ladenstein, R., Jörnvall, H. and Oppermann, U. (2002). Critical residues for structure and catalysis in short-chain dehydrogenases/reductases. J. Biol. Chem. 277, 25677–25684.
83 Kvassman, J. and Pettersson, G. (1980). Unified mechanism for proton-transfer reactions affecting the catalytic activity of liver alcohol dehydrogenase. Eur. J. Biochem. 103, 565–575.
84 Dalziel, K. and Dickinson, F. M. (1966). Substrate activation and inhibition in coenzyme-substrate reactions. Cyclohexanol oxidation catalysed by liver alcohol dehydrogenase. Biochem. J. 100, 491–500.
85 Irwin, A. J., Lok, K. P., Huang, K. W. C. and Jones, J. B. (1978). Enzymes in organic-synthesis: influence of substrate structure on rates of horse liver alcohol dehydrogenase-catalyzed oxidoreductions. J. Chem. Soc. Perkin Trans. 1, 1636–1642.
86 Theorell, H. and Chance, B. (1951). Studies on liver alcohol dehydrogenase. Acta Chem. Scand. 5, 1127–1144.
87 Dalziel, K. (1963). Kinetic studies of liver alcohol dehydrogenase and pH effects with coenzyme preparations of high purity. J. Biol. Chem. 238, 2850–2858.
88 Theorell, H., Nygaard, A. P. and Boennichsen, R. (1955). Studies on liver alcohol dehydrogenase. Acta Chem. Scand. 9, 1148–1165.
89 Shore, J. D., Gutfreund, H., Brooks, R. L., Santiago, D. and Santiago, P. (1974). Proton equilibria and kinetics in the liver alcohol dehydrogenase reaction mechanism. Biochemistry 13, 4185–4191.
90 Pettersson, G. (1987). Liver alcohol dehydrogenase. CRC Crit. Rev. Biochem. 21, 349–89.
91 Eklund, H., Samama, J.-P. and Jones, A. T. (1984). Crystallographic investigations of nicotinamide adenine dinucleotide binding to horse liver alcohol dehydrogenase. Biochemistry 23, 5982–5996.
92 Ramaswamy, S., Eklund, H. and Plapp, B. V. (1994). Structures of horse liver alcohol dehydrogenase complexes with NAD^+ and substituted benzyl alcohols. Biochemistry 33, 5230–5237.
93 LeBrun, L. A., Park, D. H., Ramaswamy, S. and Plapp, B. V. (2004). Participation of histidine-51 in catalysis by horse liver alcohol dehydrogenase. Biochemistry 43, 3014–3026.
94 Berisio, R., Lamzin, V. S., Sica, F., Wilson, K. S., Zagari, A. and Mazzarella, L. (1999). Protein titration in the crystal state. J. Mol. Biol. 292, 845–854.
95 Watt, E. D., Shimada, H., Kovrigin, E. L. and Loria, J. P. (2007). The mechanism of rate-limiting motions in enzyme function. Proc. Natl. Acad. Sci. USA. 104, 11981–11986.
96 Long, M., Betrán, E., Thornton, K. and Wang, W. (2003). The origin of new genes: glimpses from the young and old. Nat. Rev. Genet. 4, 865–875.
97 Zhang, J., Dean, A. M., Brunet, F. and Long, M. (2004). Evolving protein functional diversity in new genes of Drosophila. Proc. Natl. Acad. Sci. USA 101, 16246–16250.
98 Atrian, S. and Gonzàlez-Duarte, R. (1985). Purification and molecular characterization of alcohol dehydrogenase from *Drosophila hydei*: conservation in the biochemical features of the enzyme in several species of *Drosophila*. Biochem. Genet. 23, 891–911.
99 Winberg, J.-O., Hovik, R. and McKinley-McKee, J. S. (1985). The alcohol dehydrogenase alleloenzymes Adh^S and Adh^F from the fruitfly *Drosophila melanogaster*: an enzymatic rate assay to determine the active-site concentration. Biochem. Genet. 23, 205–216.
100 Retzios, A. (1982) Studies on *Drosophila Adh*. ÜjD thesis, University of Edinburgh, Edinburgh.
101 McElfresh, K. C. and McDonald, J. F. (1986). The effect of temperature on biochemical and molecular properties of *Drosophila* alcohol dehydrogenase. Biochem. Genet. 24, 873–889.

102 Winberg, J.-O. (1989) Biochemical and enzymological studies of some *Drosophila* alcohol dehydrogenasese, Doctoral thesis, Oslo University, Oslo.
103 Chambers, G. K., Wilks, A. V. and Gibson, J. B. (1984). Variation in the biochemical properties of *Drosophila* alcohol dehydrogenase allozymes. Biochem. Genet. 22, 153–168.
104 Horer, S., Stoop, J., Mooibroek, H., Baumann, U. and Sassoon, J. (2001). The crystallographic structure of the mannitol 2-dehydrogenase NADP+ binary complex from Agaricus bisporus. J. .Biol. Chem. 276, 27555–27561.
105 Ghosh, D., Pletnev, V. Z., Zhu, D. W., Wawrzak, Z., Duax, W. L., Pangborn, W., Labrie, F. and Lin, S. X. (1995). Structure of human estrogenic 17β-hydroxysteroid dehydrogenase at 2.2Å resolution. Sructure 3, 503–513.
106 Liao, D., Basarab, G. S., Gatenby, A. A., Valent, B. and Jordan, D. B. (2001). Structures of trihydroxynaphthalene reductase-fungicide complexes. Implications for structure-based design and catalysis. Structure 9, 19–28.
107 Hosfield, D. J., Wu, Y., Skene, R. J., Hilger, M., Jennings, A., Snell, G. P. and Aertgeerts, K. (2005). Conformational flexibility in crystal structures of human 11beta-hydroxysteroid dehydrogenase type I provide insights into glucocorticoid interconversion and enzyme regulation. J. Biol. Chem. 280, 4639–4648.
108 Yamamoto, K., Kurisu, G., Kusunoki, M., Tabata, S., Urabe, I. and Osaki, S. (2001). Crystal structure of glucose dehydrogenase from Bacillus megaterium IWG3 at 1.7 A resolution. J. Biochem. 129, 303–312.
109 Marti-Renom, M. A., Pieper, U., Madhusudhan, M. S., Rossi, A., Eswar, N., Davis, F. P., Al-Shahrour, F., Dopazo, J. and Sali, A. (2007). DBAli tools: mining the protein structure space. Nucleic Acids Res. 35, W393–397.
110 Ramaswamy, S., Scholze, M. and Plapp, B. V. (1997). Binding of formamides to liver alcohol dehydrogenase. Biochemistry 36, 3522–3527.
111 DeLano, W. L. (2002) The PyMOL User's Manual. DeLano Scientific, San Carlos, CA.
112 Krissinel, E. and Henrick, K. (2004). Secondary-structure matching (SSM), a new tool for fast protein structure alignment in three dimensions. Acta Crystallogr. 60, 2256–2268.
113 Emsley, P. and Cowtan, K. (2004). Coot: model-building tools for molecular graphics. Acta Cryst. Sect. D 60, 2126–2132.
114 Carson, M. (1987). Ribbon models of macromolecules. J. Mol. Graphics 5, 103–106.